

Hadronic Light-by-Light Scattering Contribution to the Muon Anomalous Magnetic Moment from Lattice QCD

Thomas Blum,^{1,2} Saumitra Chowdhury,¹ Masashi Hayakawa,^{3,4} and Taku Izubuchi^{5,2}

¹*Physics Department, University of Connecticut, Storrs, Connecticut 06269-3046, USA*

²*RIKEN BNL Research Center, Brookhaven National Laboratory, Upton, New York 11973, USA*

³*Department of Physics, Nagoya University, Nagoya 464-8602, Japan*

⁴*Nishina Center, RIKEN, Wako, Saitama 351-0198, Japan*

⁵*Physics Department, Brookhaven National Laboratory, Upton, New York 11973, USA*

(Received 18 July 2014; published 7 January 2015)

The most compelling possibility for a new law of nature beyond the four fundamental forces comprising the standard model of high-energy physics is the discrepancy between measurements and calculations of the muon anomalous magnetic moment. Until now a key part of the calculation, the hadronic light-by-light contribution, has only been accessible from models of QCD, the quantum description of the strong force, whose accuracy at the required level may be questioned. A first principles calculation with systematically improvable errors is needed, along with the upcoming experiments, to decisively settle the matter. For the first time, the form factor that yields the light-by-light scattering contribution to the muon anomalous magnetic moment is computed in such a framework, lattice QCD + QED and QED. A nonperturbative treatment of QED is used and checked against perturbation theory. The hadronic contribution is calculated for unphysical quark and muon masses, and only the diagram with a single quark loop is computed for which statistically significant signals are obtained. Initial results are promising, and the prospect for a complete calculation with physical masses and controlled errors is discussed.

DOI: 10.1103/PhysRevLett.114.012001

PACS numbers: 12.38.Gc, 12.20.-m, 12.38.-t, 13.40.Eh

Introduction.—The muon anomalous magnetic moment, or anomaly $a_\mu = (g_\mu - 2)/2$, provides one of the most stringent tests of the standard model because it has been measured to great accuracy (0.54 ppm) [1] and calculated to even better precision [2–4]. At present, the difference observed between the experimentally measured value and the standard model prediction ranges between $249(87) \times 10^{-11}$ and $287(80) \times 10^{-11}$, or about 2.9 to 3.6 standard deviations [2–4]. In order to confirm such a difference, which then ought to be accounted for by new physics, new experiments are under preparation at Fermilab (E989) and J-PARC (E34), aiming for an accuracy of 0.14 ppm. This improvement in the experiments, however, will not be useful unless the uncertainty in the theory is also reduced.

Table I summarizes the contributions to a_μ from QED [2], electroweak (EW) [5], and QCD sectors of the standard model. The uncertainty in the QCD contribution saturates the theory error. The precision of the leading-order (LO) hadronic vacuum polarization (HVP) contribution requires subpercent precision on QCD dynamics, reached using a dispersion relation and either the experimental production cross section for hadrons ($+\gamma$) in e^+e^- collisions at low energy or the experimental hadronic decay rate of the τ lepton with isospin breaking taken into account. Meanwhile, lattice QCD calculations of this quantity are improving rapidly [8] and will provide an important cross-check.

Unlike the case for the HVP, it is difficult, if not impossible, to determine the hadronic light-by-light

scattering (HLbL) contribution (Fig. 1), $a_\mu(\text{HLbL})$, from experimental data and a dispersion relation [9,10]. So far, only model calculations have been done. The uncertainty quoted in Table I was estimated by the “Glasgow consensus” [7]. Note that the size of $a_\mu(\text{HLbL})$ is the same order as the current discrepancy between theory and experiment. Thus, a first principles calculation, which is systematically improvable, is strongly desired for $a_\mu(\text{HLbL})$. In this Letter we present the first result for the magnetic form factor yielding $a_\mu(\text{HLbL})$ using lattice QCD.

Nonperturbative QED method.—We start by observing the difficulty computing $a_\mu(\text{HLbL})$ using lattice QCD and then explain our strategy to overcome it. Figure 1 shows two (of seven) types of diagrams, classified according to how photons are attached to the quark loop(s). In the lattice

TABLE I. The standard model contributions to the muon $g_\mu - 2$, scaled by 10^{10} . For the LO HVP, three results obtained without (first two) and with (last) $\tau \rightarrow$ hadrons are shown.

QED	up to $O(\alpha^5)$	116 584 71.8 951 (9)(19)(7)(77)	[2]
EW	$O(\alpha^2)$	15.4 (2)	[5]
QCD	LO HVP $O(\alpha^2)$	692.3 (4.2)	[3]
		694.91 (3.72) (2.10)	[4]
		701.5 (4.7)	[3]
	NLO HVP $O(\alpha^3)$	−9.84 (6)(4)	[4,6]
	HLbL $O(\alpha^3)$	10.5 (2.6)	[7]
	NNLO HVP $O(\alpha^4)$	1.24 (1)	[6]

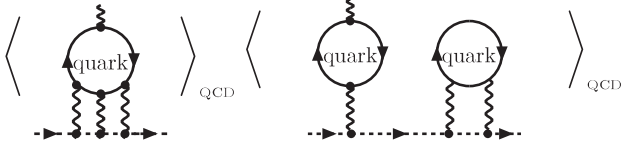


FIG. 1. Two classes of diagrams contributing to a_μ (HLbL). On the left, all QED vertices lie on a single quark loop. The right diagram is one of six diagrams where QED vertices are distributed over two (three, or four) quark loops. We refer to these as (quark) connected and disconnected diagrams, respectively.

calculation, the computation of the vacuum expectation value of an operator involving quark fields requires the inversion of the quark Dirac operator $D_{m_q}[U^{\text{QCD}}]$ for each gluon field (QCD configuration), U^{QCD} . The cost of inversion of this operator for every pair of source and sink points on the lattice is prohibitive since it requires solving

the linear equation $D_{m_q}[U^{\text{QCD}}]x_r = b_r$ for N_{sites} number of sources b_r , where N_{sites} is the total number of lattice points. In most problems, such as hadron spectroscopy, all of these inversions are not necessary. For our problem, the correlation of four electromagnetic currents must be computed for all possible values of two independent four-momenta. This implies $(3 \times 4 \times N_{\text{sites}})^2$ separate inversions, per QCD configuration, quark species, and four-momentum of the external photon to calculate the connected diagram in Fig. 1, which is astronomical. Therefore, a practical method with substantially less computational cost is indispensable.

A nonperturbative QCD + QED method that treats the photons and muon on the lattice along with the quarks and gluons has been proposed as such a candidate by us. To obtain the result for the diagram in Fig. 1, the following quantity is computed [11],

$$\begin{aligned} & \langle \psi(t', \mathbf{p}') j_\mu(t_{\text{op}}, \mathbf{q}) \bar{\psi}(0, \mathbf{p}) \rangle_{\text{HLbL}} \\ &= - \sum_{q=u,d,s} (Q_q e)^2 \sum_{\mathbf{y}} e^{i\mathbf{q} \cdot \mathbf{y}} \frac{1}{L^3 T} \sum_{\mathbf{k}} \sum_{\mathbf{z}} e^{-i\mathbf{k} \cdot \mathbf{z}} \sum_{\mathbf{x}} e^{i\mathbf{k} \cdot \mathbf{x}} \\ & \times \left\{ \left\langle \text{Tr} \{ \gamma_\mu S_q(t_{\text{op}}, \mathbf{y}; \mathbf{z}) \gamma_\nu S_q(\mathbf{z}; t_{\text{op}}, \mathbf{y}) \} \times \frac{\delta_{\nu\rho}}{\hat{k}^2} G(t', \mathbf{p}'; \mathbf{x}) \gamma_\rho G(\mathbf{x}; 0, -\mathbf{p}) \right\rangle_{\text{QCD+QED}} \right. \\ & \left. - \langle \text{Tr} \{ \gamma_\mu S_q(t_{\text{op}}, \mathbf{y}; \mathbf{z}) \gamma_\nu S_q(\mathbf{z}; t_{\text{op}}, \mathbf{y}) \} \rangle_{\text{QCD+QED}} \frac{\delta_{\nu\rho}}{\hat{k}^2} \langle G(t', \mathbf{p}'; \mathbf{x}) \gamma_\rho G(\mathbf{x}; 0, -\mathbf{p}) \rangle_{\text{QED}} \right\}, \end{aligned} \quad (1)$$

where ψ annihilates the state with muon quantum numbers, and j_μ is the electromagnetic current (the point split, exactly conserved, lattice current is used for the internal vertices while the local current is inserted at the external vertex). k is a Euclidean four-momentum, and \mathbf{p} is a three-momentum, each quantized in units of $2\pi/L$. $\delta_{\mu\nu}/\hat{k}^2$ [$\hat{k}_\mu \equiv 2 \sin(k_\mu/2)$] is the momentum space lattice photon propagator in Feynman gauge. $L^3 T$ is the space-time size of the lattice, S_q and G are quark and muon propagators, respectively, and spin and color indices have been suppressed. One takes $t' \gg t_{\text{op}} \gg 0$ to project onto the muon ground state

$$\begin{aligned} & \lim_{t' \gg t_{\text{op}} \gg 0} \langle \psi(t', \mathbf{p}') j_\mu(t_{\text{op}}, \mathbf{q}) \bar{\psi}(0, \mathbf{p}) \rangle_{\text{HLbL}} \\ &= \frac{\langle 0 | \psi(0, \mathbf{p}') | \mathbf{p}', s' \rangle}{2E'V} \langle \mathbf{p}', s' | j_\mu | \mathbf{p}, s \rangle \frac{\langle \mathbf{p}, s | \bar{\psi}(0, \mathbf{p}) | 0 \rangle}{2EV} \\ & \times e^{-E'(t' - t_{\text{op}})} e^{-Et_{\text{op}}}, \end{aligned} \quad (2)$$

where the matrix element $\langle \mathbf{p}', s' | j_\mu | \mathbf{p}, s \rangle$ is parametrized, up to muon wave function renormalization factors, as

$$-\bar{u}(\mathbf{p}', s') \left(F_1(q^2) \gamma_\mu + i \frac{F_2(q^2)}{2m_\mu} \frac{[\gamma_\mu, \gamma_\nu]}{2} q_\nu \right) u(\mathbf{p}, s). \quad (3)$$

$u(\mathbf{p}, s)$ is a Dirac spinor, and $q = p' - p$ is the spacelike four-momentum transferred by the photon. The minus sign in Eq. (3) results from the definition $F_1(0) = 1$ and the fact that the muon has charge -1 in units of $e > 0$. To extract the form factors F_1 and F_2 , Eq. (1) is traced over spins after multiplication by one of the projectors, $(1 + \gamma_t)/4$ or $i(1 + \gamma_t)\gamma_j\gamma_k/4$, where $j, k = x, y, z$ and $k \neq j$. The contribution to the anomaly is then found from $a_\mu \equiv (g_\mu - 2)/2 = F_2(0)$.

For now, quenched QED (q-QED) is used for the QED average in Eq. (1), implying no fermion-antifermion pair creation or annihilation via the photon. Note that only the sea quarks need to be charged under U(1); the lepton vacuum polarization corresponds to higher order contributions, which we ignore. This approximation was chosen to make this first calculation computationally easier, even though it is incomplete. We can remove it to get the complete physical result, as discussed at the end of this Letter. The first term, expanded in q-QED, can be reorganized as in Fig. 2, according to the number of photons exchanged between the quark loop and the open muon line. If the second term in Eq. (1) is subtracted, the connected diagram in Fig. 1, times 3 (the multiplicity arises because two of the three internal photon lines are generated three ways), emerges as the leading-order contribution in α .

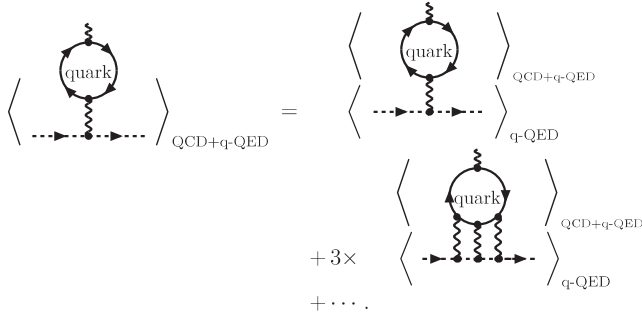


FIG. 2. Perturbative expansion of the first term in Eq. (1) with respect to QED. The symbols $\langle \cdot \rangle_{\text{QCD}+\text{q-QED}}$ and $\langle \cdot \rangle_{\text{q-QED}}$ represent the average over QCD + QED configurations (U^{QCD} , A^{QED}) and that over A^{QED} , respectively. Terms represented by the ellipsis contain four or more internal photons, and so their orders are higher than α^3 .

The main challenge in the nonperturbative method is the subtraction of the leading, unwanted components (α for the electric form factor and α^2 for the magnetic). Note that the two terms in Eq. (1) differ only by way of averaging. Thus, the cancellation of the unwanted contributions between them occurs because they are so highly correlated with respect to the QCD and QED configurations used in the averaging. Notice that all contributions from one-photon exchange between the lepton (quark) loop and muon line are canceled by the subtraction. However, two photon exchange contributions, which vanish by Furry's theorem after averaging over gauge fields, cannot appear in the subtraction term and are a potential source of large statistical errors. Fortunately, these too can be completely eliminated on each gauge configuration by switching the sign of the external momentum. This is because the projected and traced correlation function in Eq. (1) obeys an exact symmetry under simultaneous $\mathbf{p} \rightarrow -\mathbf{p}$ and $e \rightarrow -e$, where the latter is done on the muon line only. If e does not flip sign, then the only change is to multiply all contributions with an even number of photons connecting the loop and line by -1 .

We first test the nonperturbative subtraction by asking if the nonperturbative QED method applied to leptons only reproduces the known value of the sixth-order leptonic light-by-light scattering contribution [12], which is given exactly by the counterpart of the connected diagram in Fig. 1.

The test calculation was done in quenched (in the pure QED case, quenching is not an approximation since the neglected vacuum polarization contributions give higher order corrections to the light-by-light scattering diagram) noncompact QED, in the Feynman gauge, using domain wall fermions (DWF). Noncompact here only refers to the generation of the photon field configurations; the photons are coupled to the fermions via the usual exponentiated link variable. The lattice size is $24^3 \times 64$ with $L_s = 8$ sites in the extra fifth dimension and domain wall height $M_5 = 0.99$.

The muon mass and the lepton mass are the same, 0.1 in lattice units, and to enhance the signal the electric charge is set to $e = 1.0$, which corresponds to $\alpha = 1/(4\pi)$ instead of $1/137$. For simplicity, we always use kinematics where the incoming muon is at rest. The form factor F_2 was computed only at the lowest nontrivial momenta $2\pi/24$ and was not extrapolated to zero. The renormalization factor of the local vector current inserted at the external vertex is not included, as its effect is $O(\alpha)$ and should be small compared to other uncertainties.

The results for several values of the time separation between the muon source and sink t_{sep} are shown in Fig. 3 (squares). The results were computed from an ensemble of 100 uncorrelated configurations and $6^3 = 216$ point source locations for the external photon vertex, which was inserted on time slice $t_{\text{op}} = 5$. The form factor shows a large excited-state contamination, presumably arising from the contribution of muon-photon states. The value for the largest separation ($t_{\text{sep}} = 32$) is still somewhat below the continuum result, $F_2(0) = 0.371(\alpha/\pi)^3$ [13]. There may be residual excited-state contamination or finite volume and lattice spacing effects. A smaller 16^3 lattice size result (triangle) is consistent, within errors, with the 24^3 result, and the lattice result also must be extrapolated to $Q^2 = 0$ before the final comparison with continuum perturbation theory.

QCD contribution.—The inclusion of QCD into the light-by-light amplitude is straightforward: simply construct combined links from the product of U(1) (QED) gauge links and SU(3) (QCD) links [14] and follow exactly the same steps, using the same code, as described in the previous subsection. We use one quenched QED configuration per QCD configuration, though different numbers of each could be beneficial and should be explored.

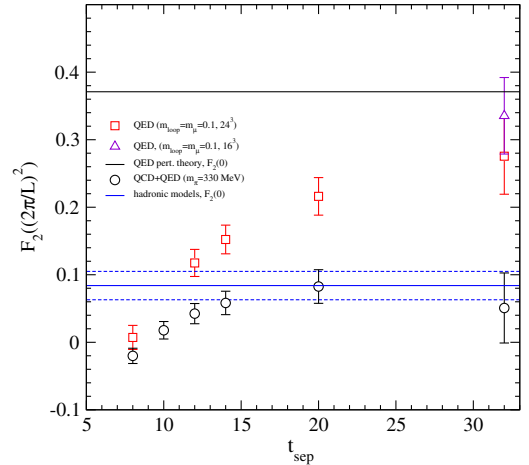


FIG. 3 (color online). The muon's magnetic form factor in units of $(\alpha/\pi)^3$ from light-by-light scattering, evaluated at the lowest nontrivial lattice momentum $2\pi/L$. Results for several symmetric source-sink separations are shown; the quark loop is the same for each and corresponds to $m_\pi = 329$ MeV (circles). Also shown is the pure QED result (squares, triangle).

Our main result is again computed on a lattice of size $24^3 \times 64$ ($L_s = 16$, $M_5 = 1.8$) with spacing $a = 0.114$ fm ($a^{-1} = 1.73$ GeV) and light quark mass 0.005 ($m_\pi = 329$ MeV) (a RBC/UKQCD collaboration 2 + 1 flavor, DWF + Iwasaki ensemble [15,16]). The bare muon mass is again set to $m_\mu = 0.1$ (the renormalized mass extracted from the two-point function is 190 MeV) and $e = 1$ as before. The domain wall height M_5 for the quark loop propagators is set to 1.8, the value used to generate the gluon gauge field ensemble; M_5 for the muon line is the same as in the pure QED case.

The all mode averaging (AMA) technique [17] is used to achieve large statistics at an affordable cost. In the AMA procedure the expectation value of an operator is given by $\langle \mathcal{O} \rangle = \langle \mathcal{O}_{\text{rest}} \rangle + (1/N_G) \sum_g \langle \mathcal{O}_{\text{approx},g} \rangle$ [17], where N_G is the number of measurements of the approximate observable, and “rest” refers to the contribution of the exact observable minus the approximation, evaluated for the same conditions. The exact part of the AMA calculation was done using 8 point sources on each of 20 configurations, and the approximation was computed using 400 low modes of the even-odd preconditioned Dirac operator and $N_G = 216$ point sources computed with stopping residual 10^{-4} on 375 configurations. On a different subset of 190 configurations, we tried 125 point sources and found the 216 sources per configuration to be more effective at reducing the statistical error. In the present calculation, the statistical errors are completely dominated by the third term in the above equation (approximately 4:1), and the correction is about $-10 \pm 5\%$.

The external electromagnetic vertex is inserted on time slice $t_{\text{op}} = 5$ with the muon created and destroyed at several time separations ranging between 8 and 20. We also include the vector current renormalization in pure QCD from Ref. [16] for the local vector current at the external vertex. We have computed the connected diagram shown in Fig. 1 for a single quark with charge +1 in the present exploratory study, so the final result is multiplied by $(2/3)^4 + (-1/3)^4 + (-1/3)^4$ to account for (degenerate) u , d , and s quark contributions.

In Fig. 3 we show $F_2((2\pi/L)^2)$ for hadronic light-by-light scattering. Again, there is a large excited-state effect; by $t_{\text{sep}} = 20$, the ground state appears to dominate. By $t_{\text{sep}} = 32$, the signal has disappeared, but there is no suggestion of large residual excited-state contamination. $F_2(Q^2)$ is shown in Fig. 4 for $t_{\text{sep}} = 10$. A similar mild Q^2 dependence is expected for other values of t_{sep} since the quark part computed in both is the same; only the muon line is different.

The value shown in Fig. 3 ($t_{\text{sep}} = 20$) is roughly consistent with the model estimate [7] using physical masses, and the statistical error is already at the same level as the model error (even larger errors appear in the literature [18]). Hadronic models with unphysical heavy masses similar to those in our study lead to a somewhat

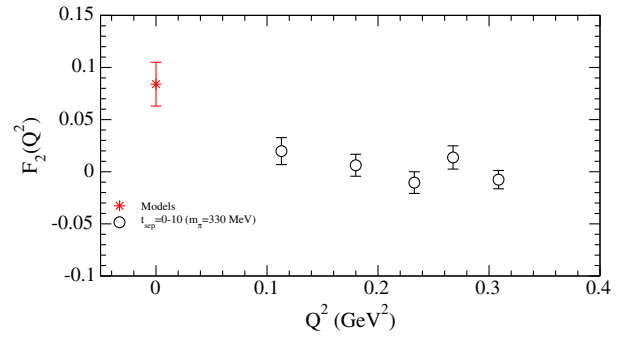


FIG. 4 (color online). The muon’s magnetic form factor in units of $(\alpha/\pi)^3$ from hadronic light-by-light scattering. $m_\pi = 329$ MeV; $t_{\text{sep}} = 10$.

higher value: in models the increase due to muon mass overwhelms the decrease due to heavier pions [19]. For example, for $m_\pi = 330$ MeV, $m_\rho = 900$ MeV, and $m_\mu = 200$ MeV, the pion exchange plus charged pion loop contributions give $8.35 - 0.51 = 7.84$ compared to $5.65 - 1.63 = 4.02$ for physical masses. η and η' exchange give similar contributions as pion exchange, so we expect that the model estimate roughly doubles from its physical point value. Extrapolation to $Q^2 = 0$ increases the lattice result, so at this stage there is no obvious conflict between the two.

As anticipated above, before averaging over equivalent external momenta, the statistical errors are considerably larger as the two-photon exchange contribution is one order lower in α . While the combinations $\pm \vec{p}$ effectively eliminate the error from this contribution, the light-by-light contribution is identical, so the statistical error is only reduced by averaging over independent momenta or the γ^μ inserted at the external vertex.

Finally, the subtraction is shown to be working properly in the (QCD + QED) case by varying e as follows. The same noncompact QED configurations are used in each case; e is varied only when constructing the exponentiated gauge link $U_\mu(x) = \exp(ieA_\mu(x))$. Thus, the ratio of form factors and, hence, the α dependence can be determined very accurately. Since one photon is inserted explicitly and the charges at the associated vertices are not included in the lattice calculation, the subtracted amplitude should behave like $e^4 \propto \alpha^2$. With the use of $e = 0.84$ and 1.19, the changes in the subtracted correlation function relative to $e = 1$ should be 0.5 and 2.0, respectively. This is what is observed numerically.

Conclusion.—The muon $g_\mu - 2$ remains the most compelling and important hint of new physics beyond the standard model. New experiments, E989 at Fermilab and J34 at J-PARC, aim to reduce the error on its measured value by a factor of 4. To eliminate the current discrepancy or elevate it to discovery of new physics requires a similar improvement in theory, which is dominated by errors from the hadronic contributions. In particular, model calculations and those based on dispersive methods [7,9,10] of

$a_\mu(\text{HLbL})$, while quite useful, do not have the required accuracy: a first principles method is needed, but has been sorely lacking.

We have presented the first lattice QCD result for the form factor that yields the hadronic light-by-light contribution to the muon anomaly. The calculation uses a nonperturbative QED method whose feasibility was first tested in the pure QED case. We have demonstrated that a statistically significant signal for the light-by-light diagram can be computed with modest statistics and that realistic results are obtained on modest size lattices. Large excited-state contamination is visible in both QED and QED + QCD, likely attributable to the same muon + photon state. With large enough time separation between the muon source and sink, results for unphysical quark and lepton masses emerge that are consistent with expectations from model calculations and QED perturbation theory. A precise calculation with physical masses, larger volume, and a controlled extrapolation to $Q^2 = 0$ is now desirable and appears feasible.

An additional systematic uncertainty in the current calculation arises from the absence of diagrams with two or more quark loops coupled to photons such as the one shown on the right in Fig. 1. This is a direct consequence of the numerical expediency of quenched QED in this first calculation. The disconnected diagram in Fig. 1 (as well as the five others not shown) is next-to-leading order in the number of colors and vanishes in the SU(3)-flavor symmetry limit. We note that all such diagrams can be included in an analogous calculation to the one presented here, but using completely unquenched QED + QCD gauge field configurations [20]. These can be dynamical QED + QCD configurations [21,22] or pure QCD ones, reweighted to nonzero electric charge [23].

We thank Norman Christ, Luchang Jin, and Christoph Lehner for useful discussions and for help checking our code against independently written code, including PHYSYCAL [24]. We also thank the USQCD Collaboration and the RIKEN BNL Research Center for computing resources. M.H. is supported in part by Grants-in-Aid for Scientific Research No. 22224003 and No. 25610053, T.B. is supported in part by the U.S. Department of Energy under Grant No. DE-FG02-13ER41989, and T.I. is supported in part by Grants-in-Aid for Scientific Research No. 22540301, No. 23105715, and No. 26400261 and also under U.S. DOE Grant No. DE-AC02-98CH10886.

- [1] G. W. Bennett *et al.* (Muon G-2 Collaboration), *Phys. Rev. D* **73**, 072003 (2006).
- [2] T. Aoyama, M. Hayakawa, T. Kinoshita, and M. Nio, *Phys. Rev. Lett.* **109**, 111808 (2012).
- [3] M. Davier, A. Hoecker, B. Malaescu, and Z. Zhang, *Eur. Phys. J. C* **71**, 1515 (2011); **72**, 1874(E) (2012).
- [4] K. Hagiwara, R. Liao, A. D. Martin, D. Nomura, and T. Teubner, *J. Phys. G* **38**, 085003 (2011).
- [5] A. Czarnecki, W. J. Marciano, and A. Vainshtein, *Phys. Rev. D* **67**, 073006 (2003); **73**, 119901(E) (2006).
- [6] A. Kurz, T. Liu, P. Marquard, and M. Steinhauser, *Phys. Lett. B* **734**, 144 (2014).
- [7] See J. Prades, E. de Rafael, and A. Vainshtein, *Lepton Dipole Moments*, edited by B. L. Roberts and W. J. Marciano, Advanced Series on Directions in High Energy Physics Vol. 20 (World Scientific, Singapore, 2010), p. 303 and references therein.
- [8] T. Blum, M. Hayakawa, and T. Izubuchi, *Proc. Sci., LATTICE 2012* (2012) 022 [arXiv:1301.2607].
- [9] V. Pauk and M. Vanderhaeghen, *Eur. Phys. J. C* **74**, 3008 (2014).
- [10] G. Colangelo, M. Hoferichter, M. Procura, and P. Stoffer, *J. High Energy Phys.* **09** (2014) 091.
- [11] M. Hayakawa, T. Blum, T. Izubuchi, and N. Yamada, *Proc. Sci., LAT 2005* (2006) 353 [arXiv:hep-lat/0509016].
- [12] J. Aldins, T. Kinoshita, S. J. Brodsky, and A. J. Dufner, *Phys. Rev. Lett.* **23**, 441 (1969); *Phys. Rev. D* **1**, 2378 (1970).
- [13] S. Laporta and E. Remiddi, *Phys. Lett. B* **265**, 182 (1991).
- [14] A. Duncan, E. Eichten, and H. Thacker, *Phys. Rev. Lett.* **76**, 3894 (1996).
- [15] C. Allton *et al.* (RBC-UKQCD Collaboration), *Phys. Rev. D* **78**, 114509 (2008).
- [16] Y. Aoki *et al.* (RBC and UKQCD Collaborations), *Phys. Rev. D* **83**, 074508 (2011).
- [17] T. Blum, T. Izubuchi, and E. Shintani, *Phys. Rev. D* **88**, 094503 (2013).
- [18] F. Jegerlehner and A. Nyffeler, *Phys. Rep.* **477**, 1 (2009).
- [19] H. Bijmns checked this for us in a model calculation for the masses used here. See also Eq. (9) in Ref. [7].
- [20] T. Blum, M. Hayakawa, and T. Izubuchi, *Proc. Sci., LATTICE 2013* (2013) 439.
- [21] R. Horsley, Y. Nakamura, D. Pleiter, P. E. L. Rakow, G. Schierholz, H. Stben, R. D. Young, and J. M. Zanotti, *Proc. Sci., Lattice 2013* (2013) 499 [arXiv:1311.4554].
- [22] S. Borsanyi, S. Durr, Z. Fodor, C. Hoelbling, S. D. Katz, S. Krieg, L. Lellouch, and T. Lippert *et al.*, arXiv:1406.4088.
- [23] T. Ishikawa, T. Blum, M. Hayakawa, T. Izubuchi, C. Jung, and R. Zhou, *Phys. Rev. Lett.* **109**, 072002 (2012).
- [24] C. Lehner, *Proc. Sci., LATTICE 2012* (2012) 126 [arXiv:1211.4013].